U-Pb and Rb-Sr isotopic study of granitic gneisses and associated metavolcanic rocks from the Rostock massifs, southern margin of the Damara Orogen: implications for lithostratigraphy of this crustal segment

N. Pfurr, H. Ahrendt, B.T. Hansen and K. Weber

Institut für Geologie und Dynamik der Lithosphäre, Goldschmidtstr. 3, D-3400 Göttingen, Germany

Rb-Sr ages and U-Pb zircon ages have been obtained for several granitic gneisses and for porphyritic rocks of an associated volcano-sedimentary unit, formerly assumed to be equivalent to the Gaub Valley Formation, in the area of the Rostock massifs situated in the Southern Margin Zone of the Damara Belt. The isotopic systems of the rocks give relevant information about the time of formation, despite relatively poor Rb-Sr and U-Pb results attributed to alteration caused by Damaran metamorphism or later uplift and erosion. Rb-Sr whole-rock data from granitic gneisses give an age of 1049 $\pm$ 28 Ma with an initial $^{87}Sr/^{86}Sr$ of 0.7061 $\pm$ 0.0002, while their U-Pb zircon data indicate a maximum age around 1200 Ma for the time of crystallisation. U-Pb zircon data of porphyritic members of the metavolcanic unit define an age around 1100 Ma for the time of crystallisation. Rb-Sr whole-rock data from mafic members within this unit provide no information about the time of formation due to metamorphic disturbance. Rb-Sr mineral systems and Rb-Sr small-scale whole-rock systems were influenced by complete resetting during Damaran metamorphism around 530-490 Ma. In general, a period of granitoid emplacement and volcanic activity between 1200-1050 Ma is indicated by the results. These rocks are consequently considered to be equivalent to the Sinclair Sequence and related intrusives. It is concluded that the emplacement of the igneous rocks is related to collision-induced rifting, complementary to the Kibaran Orogenesis.

Introduction

The Damara Belt represents the NE-trending, 400 km wide, intracontinental branch of the Pan-African Damara Orogen in Namibia. Sediments of the Damaran syncline consist of low- to high-grade metamorphic, upper-Proterozoic sedimentary and volcanic rocks correlated with the Damara Sequence (SACS, 1980). Several structural zones can be recognised within the intracontinental branch on the basis of stratigraphic, structural, metamorphic and geochronological data (Martin & Porada, 1977; Miller, 1983). According to this subdivision, the study area is situated in the Southern Margin Zone, which is defined as a 25 to 55 km wide belt of low-angle thrust sheets and southeast vergent fold nappes that consist essentially of multiply deformed Damaran cover rocks and intensely refoliated pre-Damaran basement rocks (Hoffmann, 1983). Owing to the lack of geochronological data within the southwestern part of the Southern Margin Zone, rocks have been mapped as pre-Damaran basement and correlated with the >1500 Ma old Rehoboth Sequence (Hill, 1975; Geological map of the Damara Orogen, 1980).

On the basis of geological and structural mapping in the area of the Rostock massifs (Pfurr *et al.*, 1987; Pfurr & Wissmann, 1988), geochronological studies were carried out on rocks formerly classified as equivalent to the Rehoboth Sequence. The results of these studies require a revision of the lithostratigraphy in the Southern Margin of the Damara Belt. This is supported by the results of structural and lithostratigraphic investigations in the neighboring Nukurus area by Böhme (pers. comm., 1990).

Geological setting and characteristics of the red granitic gneisses and associated metavolcanics

The Rostock massifs form a number of inselbergs of up to 5 km in diameter which rise 750 m above the desert plain of the Namib, 160 km southwest of the city of Windhoek in central Namibia. They are build up in the core of a dome structure by several thrust sheets of orthogneisses, considered to be equivalent to the pre-Damaran Gamsberg Granite (Hill, 1975), and a suite of metavolcanic and metasedimentary rocks, formerly believed to be equivalent to the pre-Damaran >1500 Ma old Gaub Valley Formation (Hill, 1975), part of the Rehoboth Sequence (SACS, 1980).

The orthogneisses are red to red-grey foliated rocks which display equigranular to porphyroblastic textures. They often carry several centimetre-sized augen-like K-feldspar blasts. Compositionally the rocks are granitic and plot in the fields of alkali feldspar granite and granite according to the classification of Streckeisen (1976). Recent analytical data (Wissmann, pers. comm., 1990) show that the red orthogneisses have the characteristics of A -type granites with a predominance of potassium, high differentiation indices and high agpaitic indices.

The volcano-sedimentary suite is composed of a succession of biotite-albite schists with intercalated porphyritic rocks, numerous basic horizons as well as albitic gneisses. The different lithologies form alternating layers of 10 cm to 10m in thickness with very sharp boundaries. In the lateral expansion of the sequence, the rock association changes to prominent mafic horizons, biotite-albite schists, garnet-amphibole-bearing chlorite-mica schists, thin dolomitic layers, albitolites and
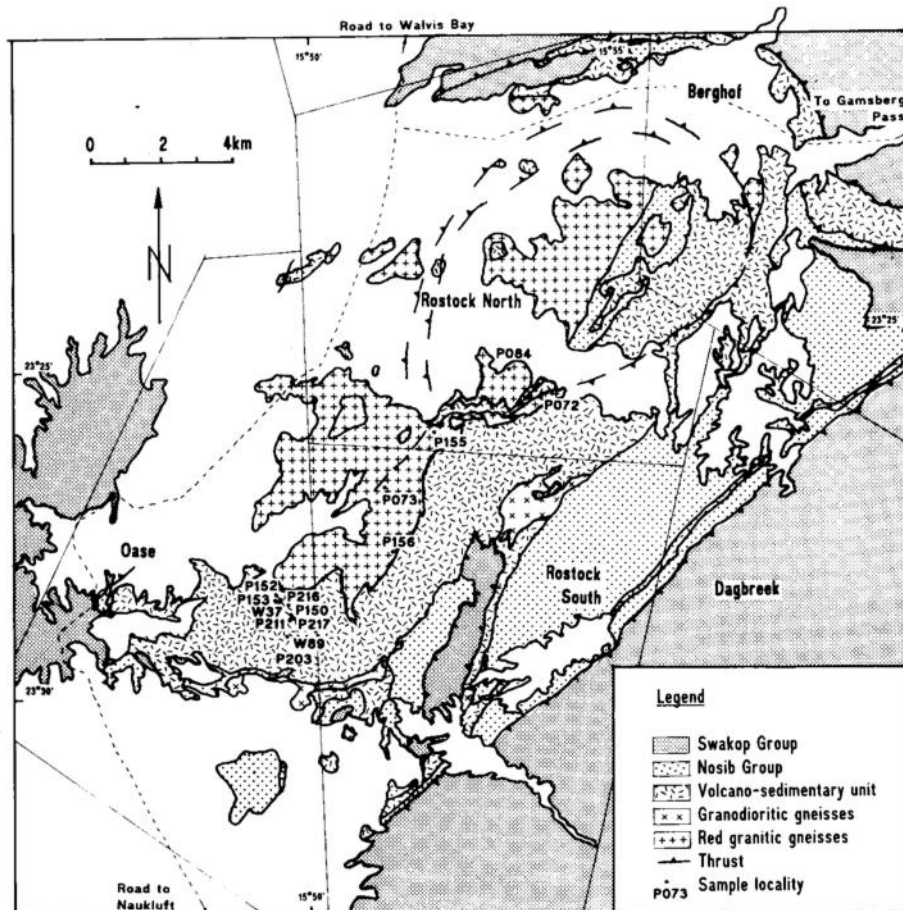
Fig. 1: Simplified geological map of the Rostock massifs modified after Pfurr & Wissmann (1988) showing sample localities.

ferruginous quartzites. Granodioritic gneisses are confined to the base of the sequence in this position.

Red, grey or dark-grey porphyritic rocks show laminated porphyroblastic textures with porphyroblasts of K-feldspar and saussuritised plagioclase as well as colourless, globular quartz up to 1 em in diameter. The mineralogical composition classifies them as rhyolitic to dacitic rocks according to Streckeisen (1976). On the basis of chemical data, Wissmann (pers. comm., 1990) has distinguished alkali rhyolite, rhyolite, rhyodacite and dacite with high Na/K ratio and high differentiation indices, and comendite with a predominance of potassium and very high differentiation indices and high agpaitic indices.

Basic horizons are represented by compact, fine-grained amphibolites consisting mainly of barroisitic hornblende, albite and a lesser content of biotite, chlorite, epidote and quartz. Schistose varieties show higher contents of biotite than the massive layers, and some horizons contain plagioclase porphyroblasts. The chemical composition classifies them as quartz tholeiitic basalts (Wissmann, pers. comm., 1990).

Partly intrusive contacts, but mainly concordant inter-fingering between the granitic gneisses and the bimodal metavolcanic suite (Pfurr *et al.*, 1987), suggest a

subvolcanic emplacement for the whole sequence similar to associations in the Karoo ring complexes in Namibia (Blümel *et al.*, 1979). Additional to the geological framework, chemical characteristics give evidence for an origin related to continental extension.

The orthogneisses and the associated volcano-sedimentary suite are overlain by Nosib Group metasediments which consist of alluvial fan deposits interfingering with rudaceous and arenaceous rocks of fluvial systems and argillaceous and carbonaceous rocks including evaporitic horizons of a sabkha playa facies. The presence of granitic, porphyritic and mafic components in mud-supported conglomerates autochthonously overlying the red orthogneisses and associated metavolcanic rocks implies a derivation of the clasts from the underlying magmatic rocks.

The Nosib Group sediments are followed by prominent dolomitic marbles associated with extraformational mud supported conglomerates grading into an interbedded sequence of alternating graded quartzite and graphite schist or several pelitic schists of the black shale facies. These units indicate subaqueous sedimentation as the result of marine transgression by increasing subsidence of the graben structure. A correlation with the basal stratigraphic units of the Swakop Group

in the sense of Hoffmann (1983) appears feasible, but no clear stratigraphic discordance between the sabkha playa facies and the marine facies is visible. The components of the stratigraphically higher conglomerate (Rostock Conglomerate) include, in addition to pebbles of underlying sediments, magmatic pebbles analogous to basal conglomerate horizons. In addition, decreasing pebble content and pebble size in the mud-supported conglomerate, as well as decreasing thickness of beds in the turbiditic sequence away from the massif, show that the magmatic rocks probably also represented the source region for the higher stratigraphic units.

The structures in the Rostock area are dominated by folding and thrusting. All lithological units comprise structural features of two major NW- and NE-trending movement phases D_1 and D_2 culminating in telescoping and imbrication of different facies units (Pfurr, 1990). The same development of both D_1 and D_2 structures in all lithological units, including the Damara Sequence, gives evidence for initiation of deformation after the deposition of the Damara Sequence. Postulated major influence of pre-Damaran tectonometamorphic processes (Kibaran Orogenesis) on the basal orthogneisses and the volcano-sedimentary suite (Hoffmann, pers. comm., 1990) can be excluded.

Rocks in the area have been regionally metamor-

TABLE 1: Rb-Sr analytical data

Sample	Concentrations		Isotopic ratios	
	Rb (ppm)	Sr (ppm)	$^{87}Rb/^{86}Sr$	$^{87}Sr/^{86}Sr$
Granitic Gneisses				
P084/WR	257	11.91	68.69	1.7229 ± 0.0008
P084/WR ra.	268	12.05	68.06	1.7229 ± 0.0002
P084/mica	926	3.78	1504	12.193 ± 0.001
P084/biotite	1477	10.55	558.0	4.4710 ± 0.0004
P072/WR	160	83.87	5.584	0.78327 ± 0.00014
P072/biotite	755	4.42	753.6	6.0700 ± 0.0026
P072/mica	413	10.28	127.1	1.6666 ± 0.0002
P073/WR	226	11.82	59.70	1.4967 ± 0.0001
P073/mica	961	4.17	1319	10.708 ± 0.001
P155/WR	127	93.03	3.970	0.76531 ± 0.0001
P156/WR	385	5.48	285.6	4.8655 ± 0.0006
P211/WR	152	57.14	7.785	0.82682 ± 0.00008
P211/biotite	931	5.48	745.2	5.9789 ± 0.0003
Porphyritic rocks				
P153/WR	83.9	54.94	4.442	0.76260 ± 0.00017
P153/WR ra.	83.8	54.70	4.457	0.76260 ± 0.00004
P153/biotite	669	3.34	967.0	7.5337 ± 0.0010
P153/WR 1 ss.	86.5	60.44	4.163	0.76126 ± 0.00007
P153/WR 2 ss.	75.7	51.65	4.261	0.76210 ± 0.00005
P153/WR 3 ss.	88.4	56.65	4.541	0.76399 ± 0.00015
P153/WR 4 ss.	94.1	56.09	4.886	0.76651 ± 0.00005
P153/WR 4 ra.	93.0	55.17	4.904	0.76651 ± 0.00005
P217/WR	51.2	247.5	0.5998	0.72095 ± 0.00005
P217/biotite	339	8.24	129.9	1.6184 ± 0.0004
P188/WR	53.9	250.1	0.6241	0.71982 ± 0.00007
P152/WR	27.8	494.6	0.1629	0.70970 ± 0.00004
Metabasalts				
P150/WR	41.3	152.8	0.7831	0.72196 ± 0.00009
P203/WR	27.2	91.21	0.8633	0.72486 ± 0.00004
P216/WR	65.6	200.3	0.9501	0.73211 ± 0.00003
36/WR	21.2	106.5	0.5783	0.72300 ± 0.00009
89/WR	39.8	131.3	0.8785	0.72878 ± 0.00007
Regression Errors			1%	0.1%

ra. = replicate analysis, ss. = small-slab samples

phosed to upper greenschist/lower amphibolite facies as indicated by perthitic exsolution in K-feldspar of felsic tuffs and the growth of white mica and biotite parallel to the gneissosity or penetrative schistosity in granitic gneisses and porphyritic rocks. Basic metavolcanics show the paragenesis of barroisitic hornblende and albite. Temperatures calculated on the basis of oxygen isotope studies of metapelitic rocks from the Rostock massifs are between 532 and 550°C (Hoernes & Hoffer, 1979).

Analytical results

Samples of granitic gneisses (40-25 kg) as well as porphyritic rocks and amphibolites of the volcanic suite (30-5 kg) were processed following procedures outlined by Teufel (1988) in order to obtain whole-rock aliquots and mica concentrates for Rb-Sr analyses and zircon concentrates for U-Pb analyses. Analytical data are given in Tables 1 and 2, the sample localities are shown in Fig. 1. Analytical work was carried out at the Zentrallaboratorium für Geochronologie at the University of Münster.

For Rb-Sr analyses, whole-rock aliquots and mica concentrates (better than 99%) were spiked with $^{84}Sr/$ ^{87}Rb mixed spike prior to dissolution. Separation of Rb and Sr was made by column chemistry using quartz columns filled with cation exchange resin (Bio-Rad AG 50 W x 8). The mass spectrometric measurements were made on a Teledyne 12"90° solid source mass spectrometer, using the tantalum double filament technique (sample loaded with triple distilled water) for the measurement of Rb and the tantalum single filament technique (sample loaded on H_2PO_4), for the measurement of Sr. The assigned analytical errors based on replicate analyses are better than 1 % for $^{87}Rb/^{86}Sr$ and 0.01 % for $^{87}Sr/^{86}Sr$. Repeated analyses of the NBS 987 standard during the course of this study gave a value of 0.71034 ± 0.00005. The calculations are based on the constants recommended by the IUGS (Steiger & Jäger, 1977). Data for Rb are corrected for mass fractionation compared to standard measurements. The least squares method of York (1969) was used for the calculation of the regression lines. All errors are given at 2σ level.

U-Pb zircon isotopic data have been obtained from four red granitic gneisses at different sample locations and from two porphyritic rocks of rhyolitic and dacitic composition in the metavolcanic suite. The zircon population was separated into fractions of different size, magnetic susceptibility and colour. The chemical procedures for the zircon analyses followed the method of Krogh (1973). To determine the concentrations, aliquots of zircon solutions were spiked with a combined, highly enriched $^{208}Pb/^{235}U$ mixed spike. U and Pb measurements were made using a rhenium single filament technique, the sample loaded with Ta_2O_5 (U) and H_3PO_4 plus silica gel (Pb). Lead isotopic data were corrected for common lead and analytical blank. For the common

lead correction, an isotopic composition was employed corresponding to the model of Cumming & Richards (1975).

For age calculations, the constants recommended by the IUGS were used (Steiger & Jäger, 1977). The errors and error correlations in the $^{206}Pb/^{238}U$ and the $^{207}Pb/^{235}U$ data were calculated according to Ludwig (1980), taking into account assigned errors to the U-Pb ratio in the spike, to the $^{207}Pb/^{204}Pb$ and $^{206}Pb/^{204}Pb$ initial, blank lead and its concentrations, that are 0.3%, 0.5%, 1 % and 100%, respectively. The correlation factor for initial and blank lead is 0.7. Resulting error ellipses for data points have been drawn at a confidence level of 95% on the concordia diagrams. Regression lines were calculated according to York (1969). Errors are given at the 2σ level.

Rb-Sr whole rock and mineral ages

Rb-Sr isotopic data calculated for seven orthogneiss samples from several outcrops in the area of the Rostock massifs (Fig. 1) define an errorchron (MSWD = 4.78) age of 1049 ± 28 Ma (Fig. 2). The initial $^{87}Sr/^{86}Sr$ ratio (Sr_i) of 0.7061 ± 0.0002 falls within the range of intermediate values which suggest that granites formed
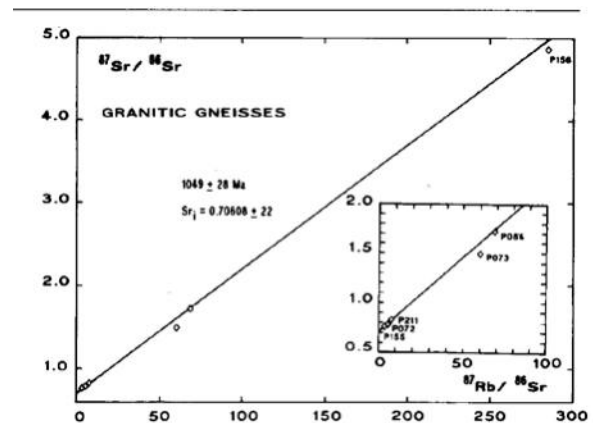

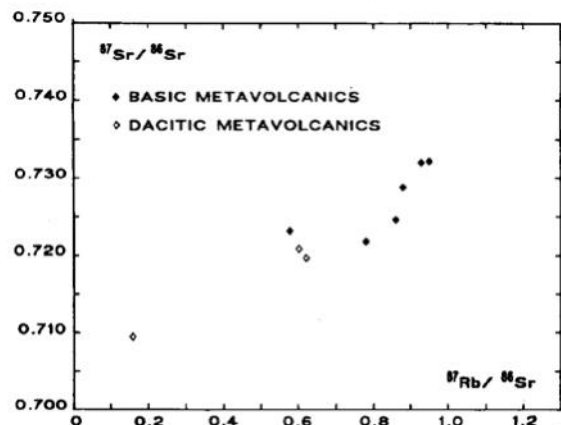**Fig. 2:** Rb-Sr isochron diagram for red granitic gneisses.

Fig. 3: Rb-Sr isochron diagram for basic and dacitic metavolcanics.

by partial melting of the lower crust or alternatively represent hybrid magmas composed of mixtures of mantle and crustal materials (Faure & Powell, 1972). The age is comparable with whole-rock data for the Gamsberg Granite in the Rehoboth-Nauchas region along the southern margin of the Damara Belt that define an errorchron (MSWD = 4.39) age of 1079 ± 25 Ma with a Sri value of 0.7081 ± 0.0012 attributed by Reid *et al.* (1988) to the time of intrusion. Seifert (1986) reported a questionable Rb-Sr whole-rock age of 1190 ± 30 Ma with a Sri value of 0.7026 ± 0.0012 for the Gamsberg pluton of the Gamsberg Granite Suite.

Data for the red granitic gneisses show that two of the samples plot below the regression line due to comparatively low $^{87}Sr/^{86}Sr$ isotope ratios. The pattern indicates disturbances of the Rb-Sr systems of the samples to different degrees that might have happened during medium-grade Damaran metamorphism. The age of 1050 Ma is consequently interpreted as a minimum age for the emplacement of the granitic rocks.

The Rb-Sr whole-rock data for the intermediate and basic metavolcanic rocks are plotted in Fig. 3 where it is clear that they do not fit an isochron. It appears probable that these rocks have become open systems to different degrees during later overprinting and cannot, therefore, provide any information about the time of formation.

Rb-Sr data of biotite-rich layers and quartz/feldspar-rich layers of a porphyritic rock of rhyolitic composition show a distinct resetting of the isotopic systems during Damaran metamorphism. The appropriate small-scale whole-rock isochron (MSWD = 0.25) defines an age of 497 ± 16 Ma with an Sri value of 0.7313 ± 0.0026 (Fig. 4).

Among the Rb-Sr isotope data for the orthogneisses and associated metavolcanic rocks, two groups of mineral ages with a difference of about 20 Ma can be recognised. The ages based on white micas form one group with values around 511 ± 2 Ma, whereas the ages of biotites give values around 491 ± 3 Ma (Fig. 5).

The interpretation of the mineral ages may take the theory of varying closure temperature (Jäger, 1979) as
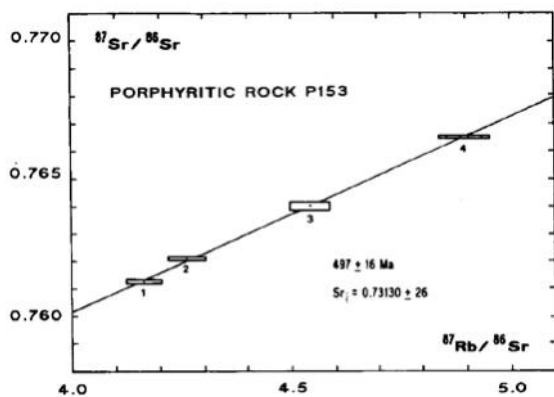
Sample	Ages in Ma ● BIOTITE ○ MICA			
	400	450	500	550
P084 GRANITIC GNEISS	●		○	
P072 GRANITIC GNEISS		●	○	
P073 GRANITIC GNEISS			○	
P211 GRANITIC GNEISS			●	
P153 PORPHYRITIC ROCK			●	
P217 PORPHYRITIC ROCK			●	

Fig. 5: Rb-Sr mineral ages of the investigated samples.

a base according to which the white mica age reflects a closing temperature of 500 ± 50°C and the biotite age reflects a closing temperature of 300 ± 50°C. In the case of medium-grade metamorphism in the rocks of the Rostock massifs, the mineral ages are thought to represent several stages of cooling with an estimated cooling rate of 7-10°C/Ma. By comparison, white mica ages in other parts of the Damara Orogen are about 20 Ma older than their corresponding biotite ages, consistent with their varying closure conditions (Blaxland *et al.*, 1979; Seifert, 1986). The peak for the regional metamorphism in lower grade metamorphic rocks in the Southern Margin Zone is defined by K-Ar mineral ages and whole rock ages of 530 Ma (Ahrendt *et al.*, 1977; Ziegler & Stoessel, 1988). By analogy with results of Seifert (1986), some biotite ages of the orthogneisses show rejuvenation with an age of 409 Ma as a result of hydrothermal activity.

U-Pb zircon ages

Zircons from the different red granitic gneisses (Table 2, Fig. 6) are heterogeneous in shape and composition. Due to the position of the samples within the gneisses, dominant zircon populations vary between normal and increasingly metamict zircons towards the margins. In addition, the uranium content of the zircon populations ranges between 300 and 3000 ppm (Table 2). The variation in uranium content in zircons of the different samples may be related to magmatic differentiation, as indicated by preliminary geochemical data (Wissmann, pers. comm., 1990). A magmatic origin for all zircons is indicated by their crystal habits, which are prismatic to long prismatic with a predominance of simple crystal faces. Pupin (1980) described comparable zircon types (D, P2-5, J5, S10-25) for hybrid granites, or granites of mainly mantle origin, with temperatures >900°C for the beginning of crystallisation. SEM and cathode luminescence studies revealed internal heterogeneities in some zircons reflecting more than one stage of crystal growth. Euhedral cores suggest a change of the growth conditions during magmatic crystallisation and a possible inherited component. Metamorphic overprinting is indicated by thin overgrown rims.

Fig. 4: Rb-Sr isochron diagram for small-scale slabs of a porphyritic rock of rhyolitic composition (P153).

TABLE 2: U-Pb analytical data for zircons from granitic gneisses and porphyritic rocks

Sample	Sieve fraction (μm)#	Concentrations			Measured ratios*			Calculated ratios+			Apparent ages (Ma)		
		U (ppm)	Pb_{ges} (ppm)	Pb_{rad} (ppm)	$^{206}Pb/^{204}Pb$	$^{207}Pb/^{206}Pb$	$^{208}Pb/^{206}Pb$	$^{206}Pb/^{238}U$	$^{207}Pb/^{235}U$	$^{207}Pb/^{206}Pb$	$^{206}Pb/^{238}U$	$^{207}Pb/^{235}U$	$^{207}Pb/^{206}Pb$
Granitic Gneiss													
P084/1	125-160	325	102.5	53.1	67	0.28642	0.69853	0.1376	1.411	0.07434	831	893	1051
P084/2	100-125	347	73.6	51.7	146	0.17186	0.42426	0.1364	1.394	0.07415	824	887	1046
P084/3	80-100	388	68.3	56.9	284	0.12436	0.31272	0.1342	1.372	0.07416	811	877	1046
P084/4	60-80	383	69.9	56.1	238	0.13353	0.33296	0.1342	1.363	0.07366	812	874	1036
P084/5	40-60	536	86.2	73.1	328	0.11657	0.27978	0.1267	1.275	0.07297	769	835	1013
P084/6	<40	435	67.0	59.1	419	0.10677	0.25689	0.1264	1.267	0.07271	767	831	1006
Granitic Gneiss													
P073/1	>160	1264	119.9	89.2	171	0.15123	0.42596	0.06285	0.5827	0.06725	393	466	846
P073/2	100-160	1484	141.8	105.2	171	0.15135	0.43135	0.06329	0.5863	0.06719	396	469	844
P073/3	60-100	1935	172.1	124.6	159	0.15622	0.43135	0.05796	0.5219	0.06531	363	426	784
P073/4	<60	2514	215.8	156.9	163	0.15153	0.40360	0.05733	0.4993	0.06317	359	411	714
P073/5	>80 c.	533	78.5	56.4	154	0.16533	0.43087	0.09537	0.9513	0.07235	587	679	996
P073/6	<80 c.	665	77.4	62.4	238	0.13219	0.35625	0.08441	0.8405	0.07222	522	619	992
Granitic Gneiss													
P156/1	31.5-60	3037	251.6	234.6	788	0.07842	0.14357	0.07745	0.6409	0.06002	481	503	604
P156/2	60-90	1813	162.7	145.4	474	0.09468	0.22596	0.07649	0.6773	0.06422	475	525	749
P156/3	90-160	2075	174.8	128.7	171	0.14857	0.35960	0.05874	0.5204	0.06426	368	425	750
P156/4	>160 m.	2338	147.2	106.2	160	0.15094	0.39547	0.04228	0.3524	0.06043	267	307	619
P156/5	125-160 m.	2421	147.0	104.6	154	0.15389	0.40131	0.04322	0.3316	0.05964	255	291	591
P156/6	90-125 m.	2972	164.1	115.9	152	0.15351	0.40507	0.03656	0.2911	0.05775	231	259	520
P156/7	60-90 m.	3135	174.8	120.2	141	0.16119	0.41361	0.03609	0.2896	0.05820	229	258	537
Granitic Gneiss													
P211/1	<50	847	93.2	78.2	296	0.12041	0.33200	0.08303	0.8250	0.07207	514	611	988
P211/2	50-90	854	88.8	75.5	324	0.11586	0.32347	0.07935	0.7847	0.07173	492	588	978
P211/3	90-125	772	85.9	68.1	224	0.13571	0.36969	0.07918	0.7817	0.07160	491	586	975
P211/4	125-160	783	84.7	66.7	217	0.13715	0.37683	0.07630	0.7502	0.07130	474	568	966
P211/5	>160	798	90.2	68.3	284	0.14783	0.40116	0.07680	0.7475	0.07059	477	567	946
P211/6	50-90 m.	910	87.3	71.4	257	0.12660	0.35552	0.07016	0.6861	0.07092	437	531	955
P211/7	125-160 m.	893	86.0	68.6	228	0.13341	0.37342	0.06858	0.6675	0.07059	428	519	946

TABLE 2: (continued)

Sample	Sieve fraction (μm)#	Concentrations			Measured ratios*			Calculated ratios+			Apparent ages (Ma)		
		U (ppm)	Pb$_{ges}$ (ppm)	Pb$_{rad}$ (ppm)	$^{206}Pb/^{204}Pb$	$^{207}Pb/^{206}Pb$	$^{208}Pb/^{206}Pb$	$^{206}Pb/^{238}U$	$^{207}Pb/^{235}U$	$^{207}Pb/^{206}Pb$	$^{206}Pb/^{238}U$	$^{207}Pb/^{235}U$	$^{207}Pb/^{206}Pb$
Porphyritic Rock													
P153/1	125 lp.	33.6	7.91	6.17	166	0.16036	0.40558	0.1668	1.719	0.07474	994	1016	1061
P153/2	90-125 lp.	159	30.2	28.1	725	0.09497	0.24835	0.1609	1.671	0.07531	962	998	1077
P153/3	>125	146	31.1	25.1	246	0.13291	0.33619	0.1570	1.624	0.07498	940	979	1068
P153/4	60-90	175	41.4	30.2	161	0.16359	0.41873	0.1554	1.612	0.07525	931	975	1075
P153/5	31.5-60	221	39.5	35.2	457	0.10572	0.28491	0.1440	1.480	0.07454	867	922	1056
P153/6	<31.5	273	45.3	41.4	567	0.09933	0.26908	0.1374	1.404	0.07415	830	891	1046
Porphyritic Rock													
P217/1	>160	174	45.1	33.3	166	0.16173	0.44706	0.1679	1.752	0.07568	1001	1028	1087
P217/2	125-160	179	52.1	34.9	124	0.19025	0.51321	0.1708	1.784	0.07577	1016	1040	1089
P217/3	80-125	186	44.2	36.4	263	0.13006	0.37721	0.1710	1.788	0.07584	1018	1041	1091
P217/4	40-80	198	42.7	38.9	543	0.10196	0.31915	0.1709	1.784	0.07572	1017	1040	1088
P217/5	<40	221	41.6	40.5	232	0.13712	0.39013	0.1608	1.683	0.07595	961	1002	1094

c. = colourless, transparent zircons, m. = zircons with low magnetic susceptibility, lp. = long-prismatic zircons

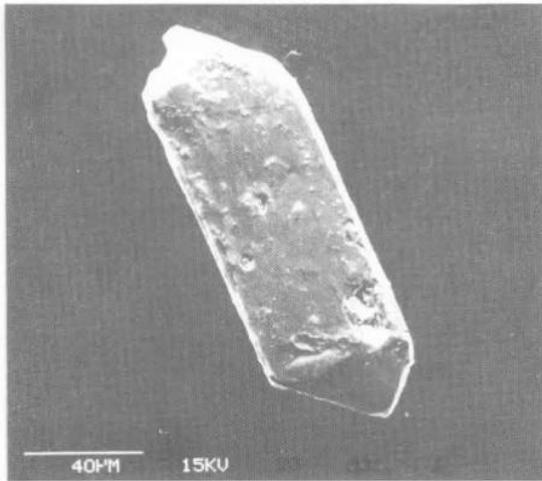* ratios corrected for mass-fractionation with a factor of 1.0012/mass unit

+ ratios corrected for blank Pb with compositions of 37.5, 15.52 and 17.72 for $^{208}Pb/^{204}Pb$, $^{207}Pb/^{204}Pb$ and $^{206}Pb/^{204}Pb$, respectively, as well as for common Pb.
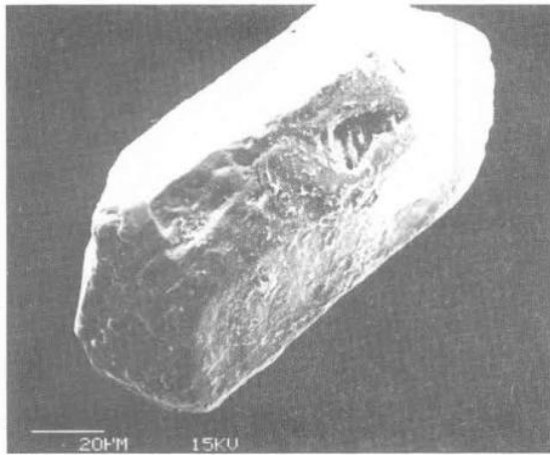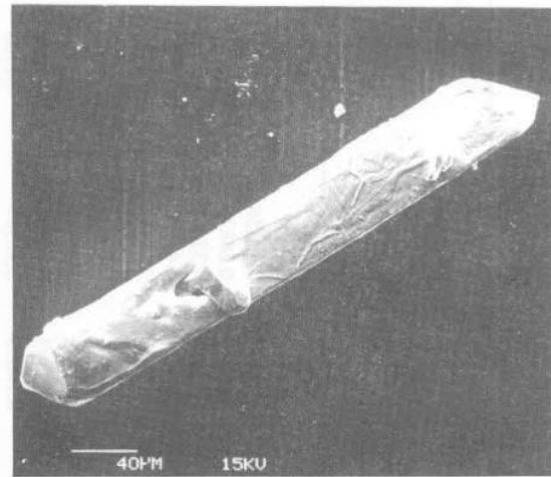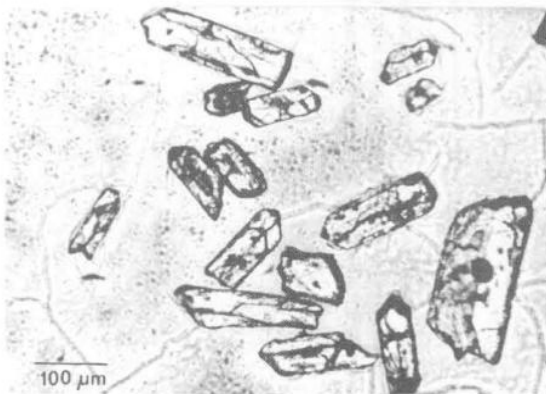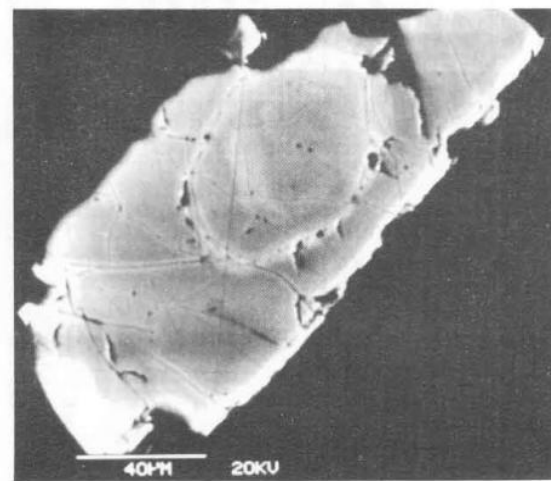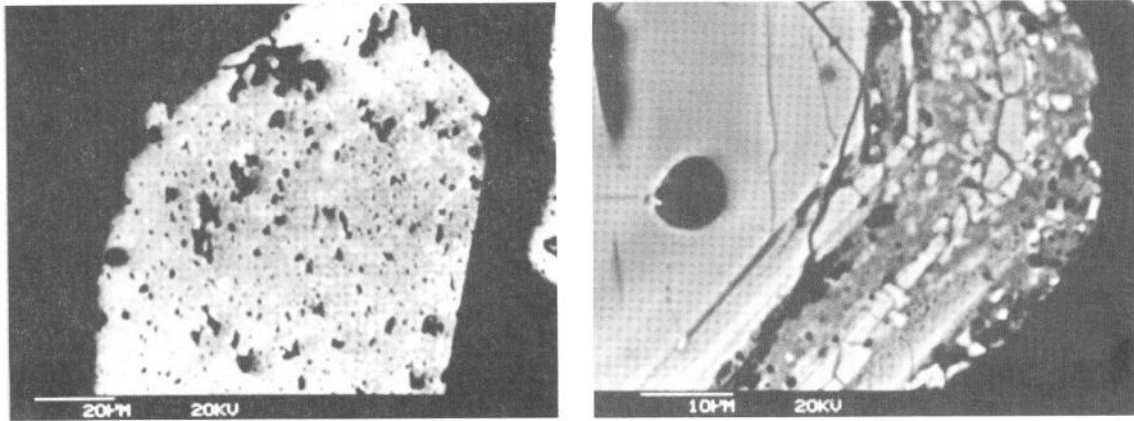
(a)
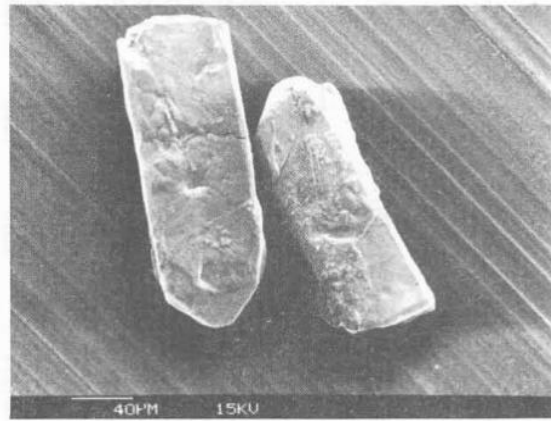
(b)

(c)

(d)

(e)

(f)

(g)

(h)

Fig. 6: Zircons of red granitic gneisses: a) SEM photograph of a malacon {110} developed as the dominant face over {100}, and weakly rounded as well as corroded surfaces (P073). b) SEM photograph of fragmented prism with thin rims of overgrowth (P084). c) SEM photograph of a prismatic malacon with simple crystal faces and slight corroded surfaces (P073). d) SEM photograph of long-prismatic, transparent zircon with small outgrowth (P073). e) Thin section under the petrographic microscope showing transparent zircons with euhedral cores of the same optical properties as well as some small turbid inclusions, with rounded contours, that are most likely inherited components. f) SEM photograph of a polished crystal, back-scattered electron mode, showing a core with rounded contours (P073). g) SEM photograph of a polished crystal, back-scattered electron mode, showing an isotropic zircon full of holes due to radiation damage (P156). h) SEM photograph of a polished crystal, back-scattered electron mode, showing a zoned crystal with holes and microchannels preferentially established in a uranium-rich outer zone (P211).
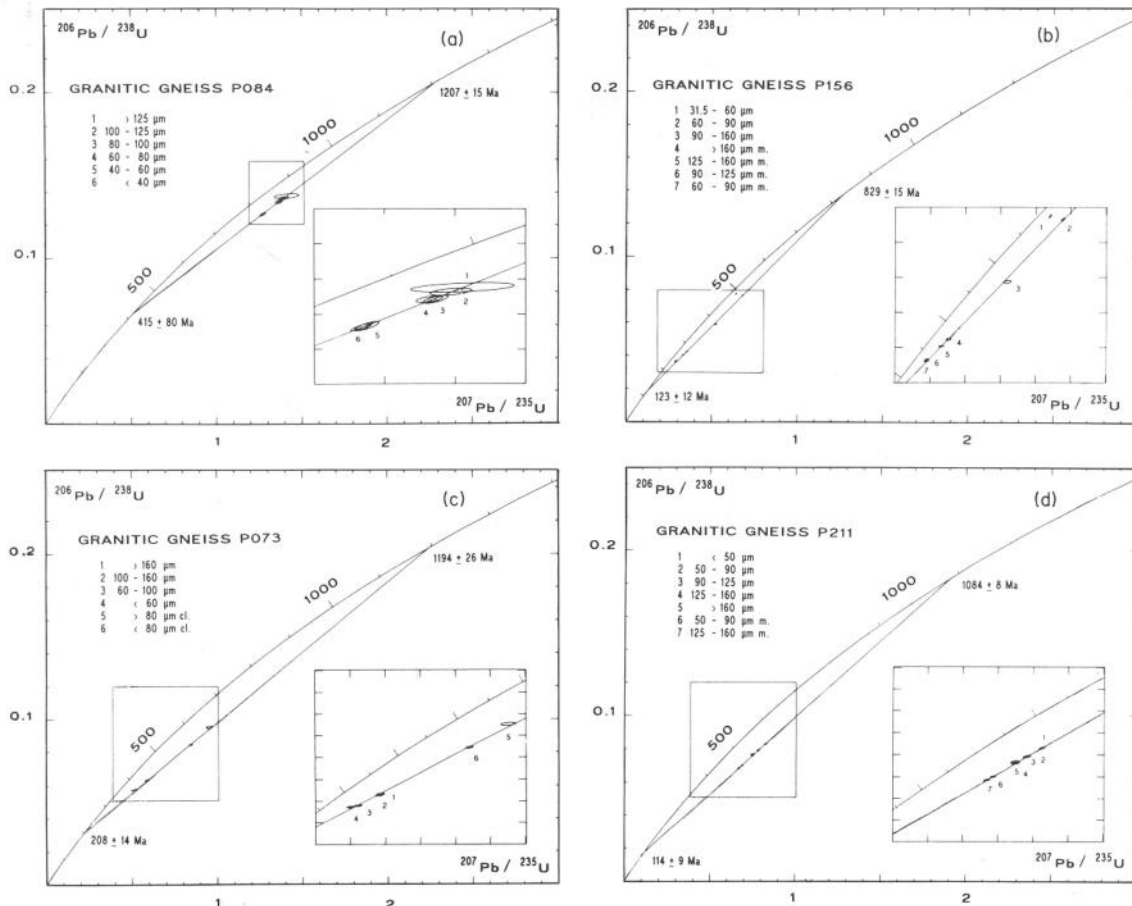

Fig. 7: Concordia diagrams for zircons from different granitic gneisses.
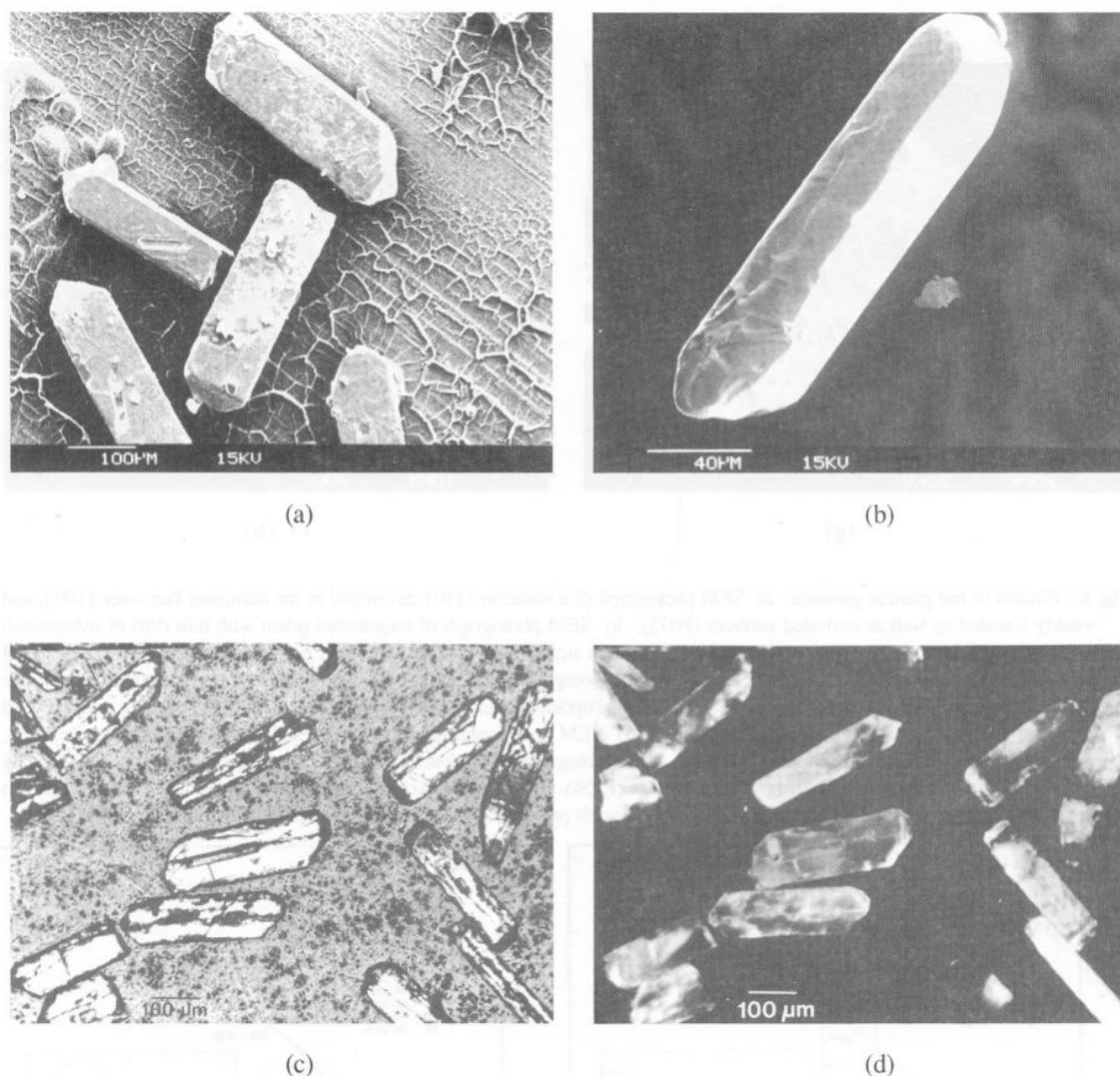
Fig. 8: Zircons of the porphyritic rocks. a) SEM photograph of fragmented prisms with simple crystal faces showing small outgrowth as well as growth disturbances (P153). b) SEM photograph of a prismatic zircon with rounded edges attributed to magmatic corrosion or metamorphic overprint (P217). c) Thin section under petrographic microscope showing prismatic zircons with inclusions of prismatic microzircons (P153). d) Cathode-luminescence photograph showing speckled luminescence pattern attributed to metamorphic recrystallisation (P153).

The U-Pb data reflect different behaviour during isotopic evolution. In concordia diagrams, the data points of the different samples define linear arrays with different grades of discordance dependent on the varying uranium content in the zircon populations (Fig. 7). The U-Pb data of zircon populations low in uranium (sample P084 in Fig. 7a) define a discordant linear pattern with an upper intercept of 1207 ± 15 Ma and a lower intercept of 415 ± 80 Ma. The U-Pb systems of zircons rich in uranium (samples P073, P211, P156 in Fig. 7b-d) yield more discordant linear patterns with upper intercept ages of 1194 ± 26 Ma, 1084 ± 8 Ma and 829 ± 15 Ma. Lower intercept ages of 208 ± 14 Ma, 114 ± 9 Ma and 123 ± 12 Ma, respectively, are better defined due to the position of data points near the lower intercept.

Zircons from porphyritic rocks of the volcano-sedimentary suite (Fig. 8) are clear to slightly pink, translucent crystals which form stubby to elongated prisms with simple pyramidal terminations. The dominant crystal habits correspond to zircon types (D, P5-4, S25-20) described for anorogenic rhyolitic rocks by Pupin (1980). Some crystals show rounded edges due to magmatic corrosion (Poldervaart, 1956) or metamorphic recrystallisation (Kalsbeek & Zwart, 1967). Cores occur in minor amounts as prismatic microcrystals.

The uranium contents of these zircons are low, ranging from 30 to 270 ppm. In a concordia diagram, data points define a linear discordance pattern with an upper intercept of 1102 ± 7 Ma and a lower intercept of 221 ± 18 Ma (Fig. 9)

Interpretation and discussion of the intercept ages

With a magmatic origin and signs of metamorphic

overprinting in the investigated zircons, the upper intercept ages of 830 and 1080 to 1207 Ma limits the time of crystallisation in relation to intrusion and eruption. On the basis of the model for episodic lead loss according to Wetherill (1956a, b), the U-Pb system should ideally yield a chord with a lower intercept representing the age of metamorphic overprinting. Metamorphism is delimited by the Rb-Sr small-scale whole-rock isochron and Rb-Sr mineral ages to a range of 530 to 490 Ma, an age range that is in agreement with metamorphic ages obtained in the southern margin of the Damara Orogen by Ahrendt *et al.* (1977), Seifert (1986) and Ziegler & Stoessel (1988).

Geologically reasonable ages are obtained only for the U-Pb zircon data for sample P084 of the red granitic gneiss. Due to the presence of a minor inherited component and poor agreement with the Rb-Sr method for the orthogneissic whole-rock systems, the upper intercept age of 1207 Ma probably reflects a maximum age of intrusion. The lower intercept age of 415 ± 80 Ma is within error of the time of metamorphism.

However, the U-Pb zircon data of the other red granitic gneisses (P073, P156, P211) display a wide range of upper intercept ages of 830, 1080 and 1194 Ma and much younger lower intercept ages of 110 to 220 Ma. Zircons with higher uranium contents plot near the low-

er intercept, which is well below the time of metamorphism in the concordia diagram. Clearly some open system behaviour occurred after the metamorphic event.

The relation between the uranium content and U-Pb ages for all investigated zircon suites show linear covariances (Fig. 10). The steep linear pattern of zircons poor in uranium can be considered as a linear function of radiation damage. In this case lead loss is controlled by radiogenic lead production dependent on the uranium content, as demonstrated by Ludwig and Stuckless (1978). In contrast, the more discordant pattern of zircon suites rich in uranium indicates their affinity to a stronger lead loss by another mechanism.

In addition, the zircon suites rich in uranium have incorporated an increasing component of common lead, expressed in the correlation of common lead to the degree of discordance and common lead to uranium (Fig. 11a, b). This signifies that the operative process in the zircons involves an exchange of common lead from elsewhere, apart from radiogenic lead loss, to which zircons rich in uranium are more susceptible (Black, 1987).

In the more radiation damaged zircons, dehydration processes are recognisable in porous surfaces as well as in disturbed, porous crystal structures (Fig. 6g, h). These structures might reflect microchannels, along which radiogenic lead could have escaped and common lead could have entered, as described by Goldich & Mudrey (1972) for lead loss correlated with uplift and the resulting reduction in confining pressure.

Exhumation of the rocks in the Rostock area in Mesozoic time is documented by apatite fission track ages of 240-115 Ma in the Gamsberg-Rostock area (Haack, 1976, 1983), by Triassic sediments of the Ka-
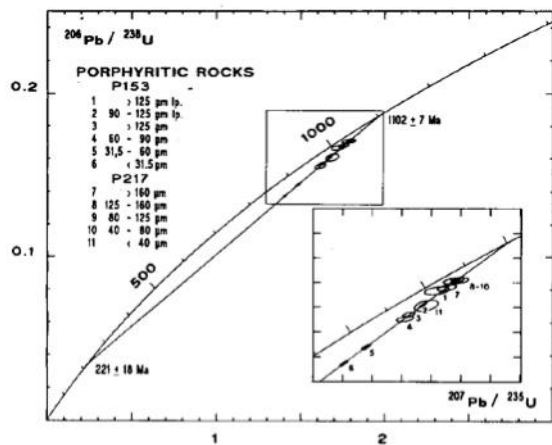

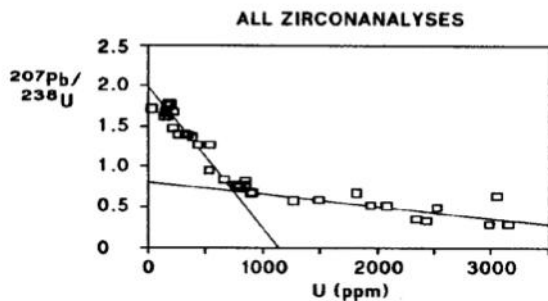Fig. 9: Concordia diagram for zircons of porphyritic rocks of the metavolcanic unit.

Fig. 10: U (ppm) vs ^{207}Pb/^{235}U diagram for all zircons (correlated with the degree of discordance). The intersects of the broken lines with the y-axis correspond to ^{207}Pb/^{235}U ages of 1150 Ma and 500 Ma, respectively.
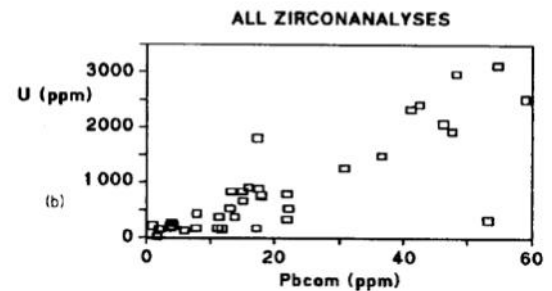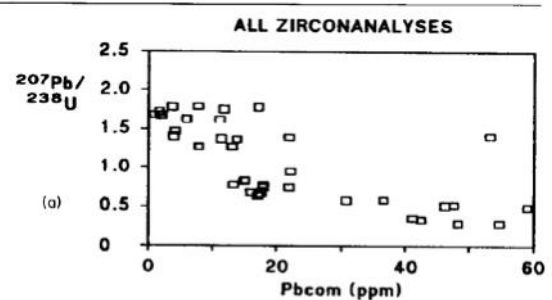

Fig. 11: a) Pbcom (ppm) vs ^{207}Pb/^{235}U diagram (negatively correlated). b) Pbcom (ppm) vs U (ppm) diagram (positively correlated).

roo Sequence unconformably overlying the Gamsberg Granite, exposed in a 1000-1500 m higher massif 60 km northeast of the Rostock massifs, as well as by Cenozoic sediments on the flanks of the Rostock massifs, deposited subsequent to tectonic instability during the break up of Gondwanaland and the opening of the South Atlantic (Ward, 1987). The break up of Gondwanaland coincided with late-Karoo ring-complexes and basaltic volcanism in Namibia, in the period 196-114 Ma (Siedener & Mitchell, 1976).

Using the above geological data, a two-stage course for the isotopic evolution of the zircons in the sense of Allègre *et al.* (1974) would provide the best explanation for the discrepancy in the U-Pb age pattern of the red granitic gneisses. The first episodic disturbance in the U-Pb systems was caused by Damaran metamorphism while the second episodic disturbance involved lead loss caused by decompression as a result of uplift and erosion.

Data points of zircon populations with a majority of non-metamict zircons from all granitic gneiss samples fit on a discordia with an upper intercept of 1210 ± 3 Ma and a lower intercept of 422 ± 3 Ma (Fig. 12), that might represent the original episodic chord for the Damaran metamorphism. The second stage opening of the U-Pb systems might possibly have rejuvenated these intercept ages. Goldich *et al.* (1970) demonstrated for the Montevideo and Morton gneisses, Minnesota, that the alignment of the U-Pb data points changed for a minimum, while the upper intercept reflects the original upper intercept age within the bounds of error. By analogy, the upper intercept of this pattern might represent the maximum age of crystallisation for zircons from the red granitic gneisses. Data points of all other zircon systems rich in uranium are also regarded to have fitted this original chord. After the second stage opening, however, zircons took up more discordant positions attributed to the higher susceptibility to further lead loss by reopening of the U-Pb systems.
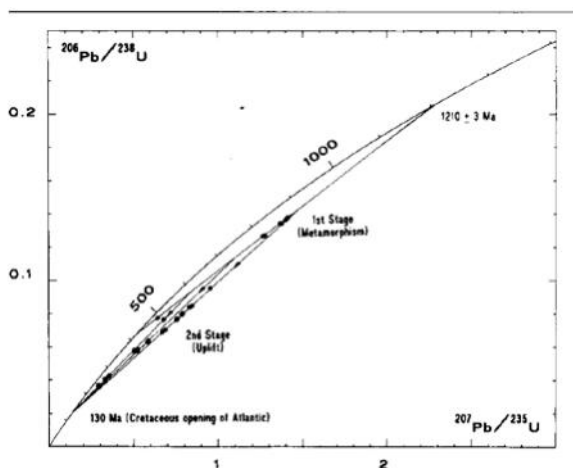

Fig. 12: Concordia diagram showing U-Pb data for all zircons from red granitic gneisses displaying a bi-episodic history.

In conclusion, a model for the isotopic evolution of zircons from red granitic gneisses is proposed with a maximum age of magmatic crystallisation around 1200 Ma, a first episodic lead loss during Damaran metamorphism and a second episodic lead loss during elevation of the rocks near surface in Triassic to Cretaceous time.

Combined with the age determined by the Rb-Sr method, U-Pb data suggest an emplacement of the granitic rocks in the period 1200-1050 Ma. Age data for the Gamsberg Granite are comparable with this result, also scattering in the range 1200-1000 Ma (Hugo & Schalk, 1972; Seifert, 1986; Reid *et al.*, 1988). According to SACS (1980) the Gamsberg Granite Suite is related to the rocks of the Sinclair Sequence.

Data for zircons from the porphyritic rocks are nearly concordant due to the very low uranium contents and the lack of a major inherited component. The upper intercept age of 1100 Ma is consequently considered to represent the time of magmatic crystallisation. Disturbance of the U-Pb systems by Damaran metamorphism is not indicated by this pattern.

The time of formation for the porphyritic rocks around 1100 Ma supports their correlation with the volcanic rocks of the Sinclair Sequence. For example, this age is indistinguishable from that reported by Hegenberger & Burger (1985) for the Oorlogsende Porphyry (1094 ± 20 Ma), which is correlated with the Nückopf Formation of the Sinclair Sequence in the northeastern extension of the southern margin of the Damara Orogen. The Oorlogsende porphyry represents the probable link to approximately 1000 Ma old volcanic rocks of an intracontinental rift in Botswana (Key & Rundle, 1981; Borg, 1988). Further comparable U-Pb age data were reported by Hugo & Schalk (1972) and in brief notes of the Geological Survey of South Africa by Burger & Coertze (1973, 1975) for acid volcanics of the Nückopf Formation along the southern margin of the Damara Orogen in the Rehoboth-Nauchas region. In addition, there is broad agreement with Rb-Sr age data reported by Hoal *et al.* (1986, 1989) for volcanic rocks of the Sinclair Sequence in the Awasib Mountain terrain.

Conclusions

Ages obtained by Rb-Sr and U-Pb studies of red granitic gneisses and a metavolcanic suite in the area of the Rostock massifs are related to a magmatic event at 1200-1050 Ma. These ages support a correlation of the orthogneissic rocks and the metavolcano-sedimentary rocks, formerly classified as Gaub Valley Formation of the Rehoboth Sequence, with the Sinclair Sequence and related intrusives that are widely distributed along the Southern Margin of the Damara Belt (Watters, 1977; Borg, 1988).

On the basis of available geological, petrographical, chemical and isotopic data, the red granitic gneisses and the associated metavolcanic rocks are interpreted as a

magmatic-sedimentary sequence related to continental rift tectonics. In the southern Damara Orogen they underlie coarse clastic and chemical continental rift sediments of the Damara Sequence, which were deposited in the onset of the down warping stage.

The time of magmatic emplacement is contemporaneous with that of the Kibaran tectogenesis that has affected the Namaqua Belt many hundreds of kilometres south of the Damara Belt 1300-1100 Ma ago (Barton & Burger, 1983). We therefore conclude that collision-induced rifting, complementary to the Kibaran orogenesis, led to the emplacement of the magmatic-sedimentary sequence of the Rostock massifs. A similar origin was proposed for igneous members of the Sinclair Sequence in the Awasib Mountain area by Hoal *et al.* (1989).

Acknowledgements

References

Ahrendt, H., Hunziker, J.C. and Weber, K. 1977. Age and degree of metamorphism and time of nappe emplacement along the southern margin of the Damara Orogen, Namibia (SW-Africa). *Geol. Rdsch.*, **67**, 719-742.

Allègre, C.L., Albarede, F., Grünfelder, M. and Köppel, V. 1974. $^{238}U/^{206}Pb$-$^{235}U/^{207}Pb$-$^{232}Th/^{208}Pb$ Zircon Geochronology in Alpine and Non-Alpine Environment. *Contr. Miner. Petrol.*, **43**, 163-194.

Barton, E.S. & Burger, A.J. 1983. Reconnaissance isotopic investigations in the Namaqua Mobile Belt and implications for Proterozoic crustal evolution - Upington Geotraverse. *Spec. Publn geol. Soc. S. Afr.*, **10**, 173-191.

Black, L.P. 1987. Recent Pb loss in zircon: a natural or a laboratory-induced phenomenon. *Chem. Geol.*, **65**, 25-33.

Blaxland, A., Gohn, E., Haack, U. and Hoffer, E. 1979. Rb/Sr ages of late tectonic granites in the Damara Orogen, SWA. *Neues Jb. Miner. Mh.*, **11**, 498-508.

Blümel, W.D., Emmermann, R. und Hüser, K. 1979. Der Erongo. Geowissenschaftliche Beschreibung und Deutung eines südwestafrikanischen Vulkankomplexes. *Scient. Res. SWA Ser., S.W. Africa scient. Soc.*, **16**, 140 pp.

Borg, G. 1988. The Koras-Sinclair-Ghanzi Rift in Southern Africa. Volcanism, sedimentation, age relationships and geophysical signature of a late Middle Proterozoic rift system. *Precambr. Res.*, **38**, 75-90.

Burger, A.J. and Coertze, F.J. 1973. Radiometric age measurements on rocks from Southern Africa to the end of 1971. *Bull. geol. Surv. S. Afr.*, **58**, 46 pp.

Burger, A.J. and Coertze, F.J. 1975. Age determinations - April 1972 to March 1974. *Ann. geol. Surv. S. Afr.*, **10**, 135-142.

Cumming, G.L. and Richards, J.R 1975. Ore lead in a continuously changing Earth. *Earth Planet. Sc. Lett.*, **28**, 155-171.

Faure, G. and Powell, J.L. 1972. *Strontium Isotope Geology*. Springer, New York, 188 pp.

Geological map of South West Africa/Namibia. 1980. Scale 1 : 1 000 000. Geol. Surv. S. Afr.

Goldich, S.S. and Mudrey, Jr. 1972. Dilatancy model for discordant U-Pb ages. *In*: *Contributions to recent geochemistry and analytical chemistry* (Vinogradow volume), Moscow: Naukla Pubis Office, 415-418.

Goldich, S.S., Hedge, C.E. and Stem, T.W. 1970. Age of the Morton and Montevideo Gneisses and related rocks, Southwestern Minnesota. *Bull. geol. Soc. Am.*, **81**, 3671-3696.

Haack, U. 1976. Rekonstruktion der Abkühlungsgeschichte des Damara Orogens in Südwest Afrika mit Hilfe von Spaltspuren-Altern. *Geol. Rdsch.*, **65**, 967-1002.

Haack, U. 1983. Reconstruction of the cooling History of the Damara Orogen by correlation of radiometric ages with geography and altitude. *In*: Martin, H. and Eder, J.W. (Eds) *Intracontinental Fold Belts - Case studies in the Variscan Fold Belt of Europe and the Damara Belt in Namibia*. Springer, Berlin, 873-884.

Hegenberger, W. and Burger, A.J. 1985. The Oorlogsende Porphyry Member, South West Africa/Namibia: its age and regional setting. *Communs geol. Surv. S.W.Africa/Namibia*, **1**, 23-29.

Hill, R.S. 1975. *Geological map 2315 BD - Rostock, scale 1:50 000*. Geol. Surv. S.W.Africa/Namibia (unpubl.).

Hoal, B.G., Harmer, RE. and Eglington, B.M. 1986. Rb-Sr geochronology of the middle to late Proterozoic Awasib Mountain Terrane. *Communs geol. Surv. S. W. Africa/Namibia*, **2**, 53-59.

Hoal, B.G., Harmer, R.E. and Eglington, B.M. 1989. Isotopic evolution of the Middle to Late Proterozoic Awasib Mountain Terrain in Southern Namibia. *Precambr. Res.*, **45**, 175-189.

Hoernes, S. and Hoffer, E. 1979. Equilibrium relations of prograde metamorphic mineral assemblages. A sTable 1sotope study of rocks of the Damara Orogen, from Namibia. *Contr. Miner. Petrol.*, **68**, 377-389.

Hoffmann, K.H. 1983. Lithostratigraphy and facies of the Swakop Group of the southern Damaran Belt,

SWA/Namibia. *Spec. Publn geol. Soc. S. Afr.*, **11**, 43-63.

Hugo, P. and Schalk, K.E.L. 1973. The isotopic age of certain granites and acid lavas in the Rehoboth and Maltahöhe District, SWA. *Ann. geol. Surv. S. Afr.*, **9**, 103-105.

Jäger, E. 1979. The Rb-Sr method, 13-26. *In*: Jäger, E. & Hunziker, J.C. (Eds), *Lectures in isotope geology*. Springer, Berlin, 329 pp.

Kalsbeek, F. and Zwaart, H.J. 1967. Zircons from some gneisses and granites in the central and eastern Pyrenees. *Geologie Mijnb.*, **46**, 1-10.

Key, R.M. and Rundle, C.C. 1981. The regional significance of new isotopic ages from Precambrian Windows through the "Kalahari Beds" in north-western Botswana. *Trans. geol. Soc. S. Afr.*, **84**, 51-66.

Krogh, T.E. 1973. A low contamination method for hydrothermal decomposition of zircon and extraction of U and Pb for isotopic age determinations. *Geochim. cosmochim. Acta*, **37**, 485-495.

Ludwig, K.R 1979. Calculation of uncertainties of U-Pb isotope data. *Earth Planet Sc. Lett.*, **46**, 212-220.

Martin, H. and Porada, H. 1977a. The intracontinental branch of the Damara Orogen in South West Africa, I. Disscussion of geodynamic models. *Precambr. Res.*, **5**, 311-338.

Martin, H. and Porada, H. 1977b. The intracontinental branch of the Damara Orogen in South West Africa, II. Discussion of relationships with the Pan-African Mobile Belt System. *Precambr. Res.*, **5**, 339-357.

Miller, R. McG. 1983. The Pan African Damara Orogen of South West Africa/Namibia. *Spec. Publn geol. Soc. S. Afr.*, **11**, 431-515.

Pfurr, N. 1990. *Die Altersstellung von Rotgneisen aus dem Rostock Deckenkomplex am Südrand des Damara Orogens, Namibia, abgeleitet aus U-Pb- und Rb-Sr-Isotopen-untersuchungen und ihre Bedeutung für die Basement-Cover-Beziehungen in der Damara Südrandzone*. Dr. rer. nat. thesis (unpubl.), Univ. Göttingen, 179 pp.

Pfurr, N., Wissmann, K., Ahrendt, H., Hill, R.S. and Weber, K. 1987. Alpinotype thrust tectonics and basement-cover relationships in the Southern Margin Zone of the Pan-African Damara Orogen, Rostock Area. *Communs geol. Surv. S.W. Africa/Namibia*, **3**, 129-136.

Pfurr, N. & Wissmann, K. 1988. *Geologische Karte 1 : 50 000; Blatt Rostock BD 2315 und Blatt Namibgrens DB 2316* (unpubl.).

Poldervaart, A. 1956. Zircons in rocks. 2. Igneous rocks.

Am. J. Sci., **254**, 521-554.

Pupin, J.P. 1980. Zircon and granite petrology. *Contr. Miner. Petrol.*, **73**, 204-220.

Reid, D.L., Mailing, S. and Allsopp, H.L. 1988. Rb-Sr ages of granitoids in the Rehoboth-Nauchas area, South West Africa/Namibia. *Communs geol. Surv. S.W. Africa/Namibia*, **4**, 19-27.

Seifert, N. 1986. Geochronologie am Siidrand des Damara-Orogens, S. W.A./Namibia: Hydrothermale Beeinflussungen von Isotopensystemen und Abkiihlalter in prakambrischen Basementgesteinen. *Schweiz. miner. petrogr. Mitt.*, **66**, 413-451.

Siedener, G. and Mitchell, J. 1976. Episodic Mesozoic volcanism in Namibia and Brazil: K-Ar isochron study bearing on the opening of the South Atlantic. *Earth Planet. Sc. Left.*, **30**, 292-302.

South African Committee for Stratigraphy (SACS), 1980. Kent, L.E. (Comp.) Stratigraphy of South Africa. Part I: Lithostratigraphy of the Republic of South Africa, South West Africa/Namibia, and the Republics of Bophutatswana. Transkei and Venda. *Handb. geol. Surv. S. Afr.*, **8**, 690 pp.

Steiger, R.H. and Jäger, E. 1977. Subcommision on geochronology: Convention on the use of decay constants in geo- and cosmochronology. *Earth Planet Sc. Lett.*, **36**, 359.

Streckeisen, A. 1976. To each plutonic rock its proper name. *Earth Sci. Rev.*, **12**, 1-34.

Teufel, S. 1988. Vergleichende U-Pb- und Rb-Sr-Altersbestimmungen an Gesteinen des Übergangsbereiches Saxothuringikum/Moldanubikum, NE-Bayem. *Göttinger Arb. Geol. Paläont.*, **35**, 87 pp.

Ward, J.D. 1987. The Cenozoic succession in the Kuiseb Valley, Namib Desert. *Mem. geol. Surv. S.W. Africa/ Namibia*, **9**, 124 pp.

Watters, B.R. 1977. The Sinclair Group: Definition and regional correlation. *Trans. geol. Soc. S. Afr.*, **80**, 9-16.

Wetherill, G.S. 1956a. An interpretation of the Rhodesia an Witwatersrand age patterns. *Geochim. cosmochim. Acta*, **9**, 290-292.

Wetherill, G.S. 1956b. Discordant uranium-lead ages, I. *Trans. Am. Geophys. Union*, **37**, 320-326.

York, D. 1969. Least-squares fitting of a straight line with correlated errors. *Earth Planet Sc. Lett.*, **5**, 320-324.

Ziegler, U.R.F. and Stoessel, G.F.U. 1988. K-Ar dating of the Marienhof and Billstein Formations in the Rehoboth Basement Inlier, SWA/Namibia. *Communs geol. Surv. S.W. Africa/Namibia*, **4**, 45-50.